

Synthesis and mechanical characterization of alumina based composite material for armor application

Muhammad Shahid^a, Rizwan Ahmed Malik^{a,*}, Hussein Alrobei^{b,*}, Jaehwan Kim^c, Muhammad Latif^c, Azhar Hussain^a, Muhammad Uzair Iqbal^a and Azeem Hafiz^b

^aDepartment of Metallurgy and Materials Engineering, University of Engineering and Technology, Taxila, 47050, Pakistan

^bDepartment of Mechanical Engineering, College of Engineering, Prince Sattam bin Abdul Aziz University, AlKharj 11942, Saudi Arabia

^cCenter for Nanocellulose Future Composites, Department of Mechanical Engineering, Inha University, 100 Inha-Ro, Michuhol-Ku, Incheon 22212, South Korea

This study focuses on development of advance ceramic with improved toughness which can be used as armor material for personnel protection. Toughness is the characteristics that defines material resistance to fracture. Ceramics are important class of materials with combination of good strength, toughness and with stand multiple-striking. In this study, three different samples i.e. alumina, Zirconia toughened alumina (ZTA), and alumina incorporated with SiC (SiCA); hexagonal shape samples were made by dry pressing and sintered at 1600 °C in argon atmosphere. Microstructural characterization: SEM and Optical microscopy demonstrated fine grain size distribution in matrix phase. BSE images confirmed the presence of ZrO₂ particles. High porosity of about 6.35% was observed in SiCA samples. EDX analysis confirms the composition. Mechanical characterization showed improved toughness at the expense of hardness. SiCA samples showed maximum value of hardness while ZTA showed maximum toughness of 4.6 MPa·m^{1/2}. The obtained properties are comparable to other ceramic materials prepared by different methods.

Keywords: Ceramic Matrix Composites, Zirconia Toughened Alumina, Dry Pressing, Mechanical Characterization.

Introduction

Engineering ceramics show excellent mechanical properties (e.g., hardness, high strength, and stiffness) over a broader range of temperatures and are suitable for high temperature applications such as fabrication processes of advance functional materials to be used in various fields i.e. electronic industry, automotive and aerospace industry etc. [1-4]. As firearms are becoming increasingly sophisticated, sufficient efforts have been made to improve armor ballistic performance, with ceramic materials at the forefront of such studies at the moment. Such initiatives focused on improving processing and reinforcing microstructure and most importantly improving toughness. Although, steel is thought to be a major material used in armor system due to its excellent mechanical properties, but lighter composites and ceramics are gaining the ground. Similarly guns now days in use are capable of producing multiple shots at a time. Therefore in case of steel multihit properties are diminishing one [5].

Al₂O₃, B₄C SiC, and ceramic matrix composites

(CMCs) such as Al₂O₃/ZrO₂ are the major ceramics materials that are commonly used for ballistic armor's production. Ceramic composite materials are presently being developed to reduce weight, price and to improve ballistic performance. The major drawbacks of ceramics armor are manufacturing hindrance, comparatively high cost and difficulty in predicting the ballistic efficiency. Fracture strength of more than 1 GPa and fracture strength of 4.7 MPa·m^{1/2} was reported [6, 7]. For that purpose many of scholars and manufacturer are working to enhance the strength and fracture toughness of ceramics but not at the expense of weight. Al₂O₃ is thought to be potential candidate for ballistic application because of its low cost to benefit ratio and ease of processing, high modulus of elasticity and high hardness [8]. However, the ballistic efficiency of alumina is lower as compared to SiC and B₄C because of poor fracture and bending strength. Such properties can be improved by addition of tetragonal zirconia/SiC/CNTs and/or developing the CMCs structures.

Zirconia toughened Alumina (ZTA) is the composite of zirconia and alumina which results improved fracture toughness and bending strength. This increased toughness is mainly because of phase transformation of zirconia from tetragonal to monoclinic associated with expansion and generation of compressive strength [9].

*Corresponding author:
E-mail: rizwanmalik48@yahoo.com (R.A. Malik)
h.alrobei@psau.edu.sa (H. Alrobei)

D. Casellas et al studied the influence of ZrO_2 particle on toughness of monolithic Al_2O_3 tiles and a ZrO_2 toughened Al_2O_3 (ZTA) composite was studied as a result of different heat treatments. It was observed that the addition of ZrO_2 particles results in an increase in the toughness of the fracture relative to that shown by the matrix of Al_2O_3 . Also microstructural coarsening within ZTA results in an increase in fracture toughness primarily associated with the impact of ZrO_2 particle size on the transformability of their stage. It was concluded that grain growth of a Al_2O_3 matrix is hindered effectively by ZrO_2 particle. Also by adding ZrO_2 particles to a Al_2O_3 matrix leads to a reduction in hardness which is associated with tetragonal ZrO_2 reduce hardness relative to Al_2O_3 . The increased transformation potential of ZrO_2 resulting from heat treatment leads to a further reduction in hardness but the toughness increases. This increase in toughness is due to the coarsening of ZrO_2 particles [10]. Tadashi Hotta et.al. Studied the effect of coarse particle on strength and microstructure of sintered alumina bodies manufactured by slip casting. Agglomerates particles were added in slurry just before casting. Fracture toughness and strength were examined [11, 12]. Penetration tests have been performed on four different ceramic materials, including alumina, modified alumina, silicon carbide and boron carbide, in support of improved personal armor protection. The results are described in terms of ballistic efficiency, and the validity of using ballistic efficiency as a measure of ceramic performance has been tested. Furthermore, the association between the properties of ballistic efficiency and ceramic materials, such as elastic modulus, hardness, spall strength and Hugoniot, Elastic Limit, was considered [13-15]. A study was made by Silva et al. [16], with the aim to find out the ballistic performance and mechanical characterization of Al_2O_3 based armor plate. Different composition varying Al_2O_3 contents were processed and sintered in furnace at $600^\circ C$ for up to 6 h and reported improved. Momohjimoh et al. [17], study focuses on the recent development in the synthesis of alumina-SiC nanocomposite which can alter the mechanical and thermal properties of alumina. Adding SiC to alumina alters the fracture mode from intergranular to transgranular as a result of grain boundary strengthen. SiC nanoparticles also inhibit grain boundary movement in alumina matrix. This refinement in microstructure by SiC addition is deemed to the unusual increase in strength and hardness of alumina SiC nanocomposite. In addition, different combinations of ceramic matrix composites were studied and effect of reinforced particles on base matrix were investigated. Nihara et.al reported that addition of SiC in alumina can enhance the fracture strength and toughness. Aluminum creep resistance was also found to increase with the addition of 5 wt percent of SiC. Fibres or nanotubes with characteristic dimensions of less than 100 nm, nanocomposite can be defined as a composite system consisting of a matrix and homogeneously dis-

persed phase particles [18]. Alumina based nanocomposite which are developed by adding suitable nanoparticles or fibres in the second phase can have improved performance in comparison to alumina, mechanically and functionally. Many other materials, have been used to reinforce alumina including titanium carbide (TiC) [19], silicon nitride (ZrO_2) [20] titanium nitride (TiN) [12] titanium oxide (TiO_2) and silicon carbide (SiC) [17]. Seung et.al proposed a novel way to manufacture CNTs reinforced alumina nanocomposite by molecular mixing method [21]. Several attempts have been made to produce CNT/alumina nanocomposite with improved hardness and toughness [22-24]. However, as mentioned earlier mechanical properties of CNT/ceramic nanocomposite are much lower than predicted or much worse than monolithic ceramics in some cases [22-25].

Badmos and Douglas et al., [26] investigated and characterized the structural Al_2O_3 ceramics for ballistic armor and wear application manufactured by slip casting and dry processing method. Characterization was done in term of fracture toughness, hardness, elastic modulus and microstructural characteristics. It was found that with increasing hardness fracture toughness decreases for a given composition. It was also noted that the samples prepared by dry processing showed lower fracture toughness and higher hardness for same Al_2O_3 percentage. In the study done by Zhang et al. [27, 28], high purity alumina was incorporated with oxides of zirconia and magnesia. Samples were then sintered and machined as per experimental scheme. Adding Al_2O_3 in alumina ceramic usually improves its toughness but decreases its hardness. Improved toughness of the ceramic, particularly in the anti-penetration phase, is much needed to have both beneficial and detrimental effect.

As ceramic materials show low density, high compression strength with good durability; these are being used extensively in aircraft frames, armor systems, tanks, and combat vehicles. However, ceramic being naturally brittle with low toughness, limits their applications. This limitation can be overcome by making ceramic matrix composite by addition of some second phase particles i.e. tetragonal zirconia, silicon carbide (SiC) nanoparticles etc. It is found that the investigation of a ceramic matrix composite comprises of alumina as a matrix material reinforced with SiC and Zirconia made by dry pressing in argon atmosphere, their microstructural study, investigation of toughness and hardness properties and their systematic comparison are a new field yet to be explored.

Methodology

Alumina was chosen as a base material because of its ease of processing. Alumina were doped with tetragonal zirconia and silicon carbide. The slip containing composition (Table 1) was first dried and were then dry

Table 1. Composition of samples.

Sample	Al ₂ O ₃	Na ₂ CO ₃	Na ₂ CO ₃	ZrO ₂	SiC
Simple	90	5	5	0	0
ZTA	87	5	5	3	0
SICA	87	5	5	0	3

pressed at 110 MPA. The pressed samples were then sintered in argon atmosphere at 1600 °C

Material selection

As discussed above by comparing the properties of most commonly used ceramic material for armor application, alumina is found to be the most suitable because of its easily process ability and comparable properties in accordance with the other two ie Boron carbide and silicon carbide. Al₂O₃ Is probably the most commonly available ballistic ceramic due to its low cost and easy availability. It has overall good ballistic efficiency even gains the tungsten core bullet and it can be used against small caliber mild steel ammunition. It can easily be found in purity ranging from 90 to 100% but the composition between 96 to 99.8% shows excellent price and performance ratio.it can also be provided with zirconia content that increases the ballistic efficiency but at the cost of density. Alumina powder was bought from a local vendor with particle size of about 6 μm.

Slip preparation

Slip was made using Alumina powder as raw material with distilled water/ethanol, binder and different additives were put in a cylindrical shell that contains manganese steel balls. In the light of the work done by researcher’s sodium carbonate was used as a binder from 3 to 5%. It was made to rotate at 68 rpm for homogenized mixing of the composition. This process was kept continued from 6 to 30 h. Three compositions were made as given in table 1, that were named as; sample containing alumina is named as Simple, sample containing ZrO₂ named as (ZTA) and samples incorporated with SiC is named as (SiCA). Slip made was then poured to plaster of Paris mold and was kept in air for 24 h for partial drying. The slip was then removed in a box upon removal of the moisture and is then processed further. After complete drying of the slip product it was then pressed to desire Shape/geometry. Pressing of ceramic powder was done using hydraulic press at 2500 psi. The pressed product has the thickness in the range of 10 mm. Green density was measured which was found quite relative to the desired one. The samples were then loaded into a vacuum sintering furnace having argon atmosphere and were sintered at 1600 °C with prescribed heating rate. The sample were given soaking time of about 6 h. The sintering cycle used was as fallows in Fig. 2.

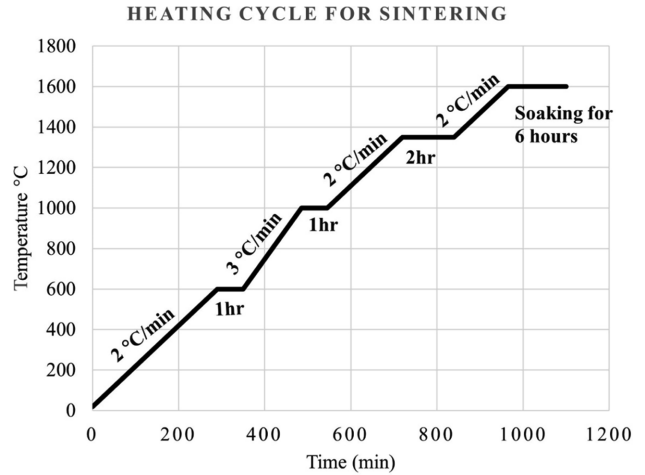


Fig. 1. Sintering cycle.

Physical properties characterization

As known, it is important to inspect and test the ceramics to ensure the final product. To check the physical properties i.e., apparent density bulk density relative density and apparent porosity were measured.

Density measurement

Density was measured by displacement method in which test specimen were suspended in water and the weight known as suspended weight (s) was measured. After this samples were taken out of the water and the dry weight was measured in air. This weight is called soaked weight (w). Bulk and the apparent density is calculated as [29, 30]

$$AP = \frac{W-D}{W-S} \times 100(\%) \tag{1}$$

Bulk density was calculated as;

$$BD = \frac{D}{W-S} - \text{density of the media} \tag{2}$$

Distilled water was used as media in this case having density of 1.00 g/cm.

Relative density was also found by the formula [30]

$$\rho_r = \frac{\rho_{ap}}{\rho_t} \tag{3}$$

Porosity measurement

Porosity was determined using equation [31]

$$E = 1 - \rho_r \tag{4}$$

Mechanical characterization

Hardness measurement

Sample Hardness was measured by Vickers hardness tester using diamond indenter. The diagonal measurement of indentation was measured by using the micrometer fixed on the machine. The results were calculated by

machine automatically. The micro hardness profile of three different types of samples were measured from center to both sides. Almost 6 indents were made on each sample after every 2 mm. The force of indentation was selected 1470N. Vickers hardness number will be determined by the following formula [32]

$$HV = 1.8544 \frac{P}{d^2} = 0.4636 \frac{P}{a^2} \quad (5)$$

Here P is the load indentation and d are the diagonal size.

It can also be calculated by

$$H = 2.0 \frac{P}{d^2} = \frac{P}{2a^2} = 0.5000 \frac{P}{a^2} \quad (6)$$

Toughness measurement

Cracks from the Vickers indentations were used to measure the fracture toughness by Anstis method. Fracture toughness was estimated by Vickers indentation method and is termed as K_c or K_{ic} fracture toughness can be calculated in $N/m^{1.5}$ using Anstis method given by Eq. (7).

$$K_{ic} = 0.016 \left(\frac{E}{H} \right)^{0.5} \cdot \left(\frac{P}{c^{1.5}} \right) \quad (7)$$

Here,

H is hardness in GPa

E is the modulus of elasticity in GPa

P is the Indentation load in N

C Crack length in m

E and H can also be written in combined form as

$$x = 0.016 \left(\frac{E}{H} \right)^{0.5} \quad (8)$$

Results and Discussion

Density and porosity measurement

True or theoretical density was measured by rule of mixture using theoretical densities of Al_2O_3 , ZrO_2 and SiC are 3.95 g/cm^3 , 5.71 g/cm^3 respectively. Density was also measured using displacement method. Density

of ZTA was found to be 4.004 g/cm^3 while that of SiCA and simple alumina was 4.1 g/cm^3 and 3.99 g/cm^3 respectively. In view of the sensitivity of density it was also measured using pycnometry and the values are given in the Table 2. Relative density as calculated using equation 3 while porosity was measured using Eq. (4). It can be seen from the table that pure alumina has the highest density value and the SiC sample has the lowest in comparison while reduced ZTA samples have the intermediate values of density and porosity so it is thought to be best suitable in view of physical and mechanical properties.

Metallography

Micrographs of Polished surfaces of the samples are shown in Fig. 2. Fig. 2(a) shows that it contains more $\alpha-Al_2O_3$ phase also the residue of sintering additives can be clearly seen in Fig. 2(b) white particles are ZrO_2 grains which are smaller and widely distributed. It shows that the ZrO_2 addition has significant effect on grain growth of ZTA. Also, as ZrO_2 act as the elongated second phase particle in ZTA so it is located at grain boundaries for crack arrest. White particles in the figure are clearly ZrO_2 . In Fig. 2(c) black particles seems to be the residue of sintering additives. But there is indication from the literature that it may act as the second phase particle to tailor the grain size and to improve densification, while the blackish region shows the porosity or sintering additives.

Scanning Electron Microscopy and EDX

SEM analysis of the samples shows morphology and surface texture as given in following figures. It was seen that Pores were widely distributed within the

Table 2. Apparent and true density with relative density and porosity measurement.

Sample	Apparent density $\rho_{AP} \text{ (g/cm}^3\text{)}$	True Density $\rho_t \text{ (g/cm}^3\text{)}$	Relative density $\rho_r \text{ (%)}$	Porosity $\epsilon \text{ (%)}$
Simple	3.75 ± 0.02	3.82	98.1	1.9
ZTA	3.42 ± 0.02	3.54	96.6	3.4
SiCA	3.25 ± 0.02	3.47	93.65	6.35

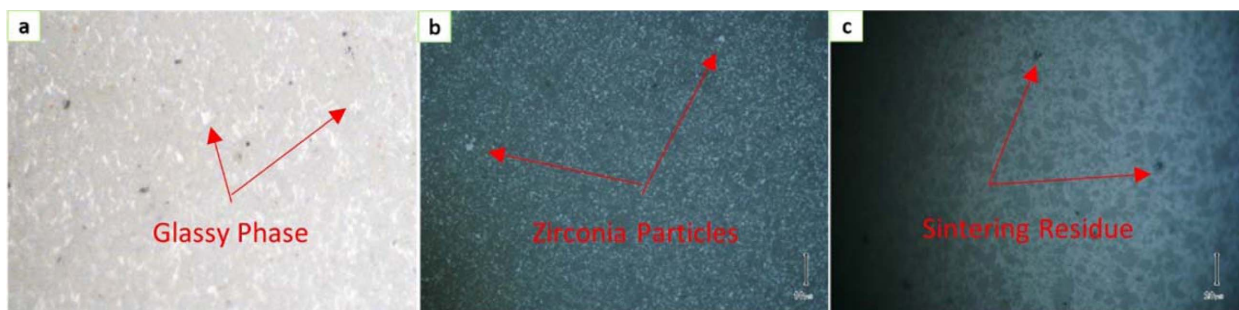


Fig. 2. Optical micrographs of simple alumina (a), ZTA (b), SiCA (c).

samples but were ideally situated at the boundaries of grains. They were different in sizes with larger pores up to 5 μm in diameter, as shown in Fig. 3-5. ZTA's

high level of porosity makes this semi-transparent to light. As the use of zirconia as second phase particle usually inhibit grain growth especially in pressure less

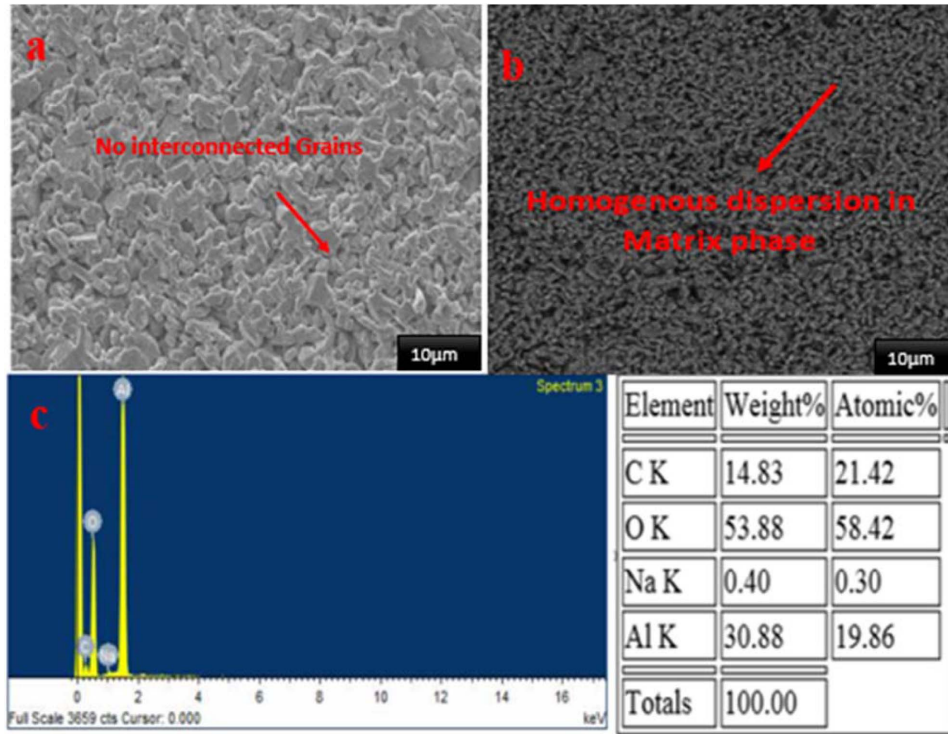


Fig. 3. SEM images and EDS Spectra shows the chemical composition of base alumina (a) SE (b) BSE (c) EDS analysis confirming composition.

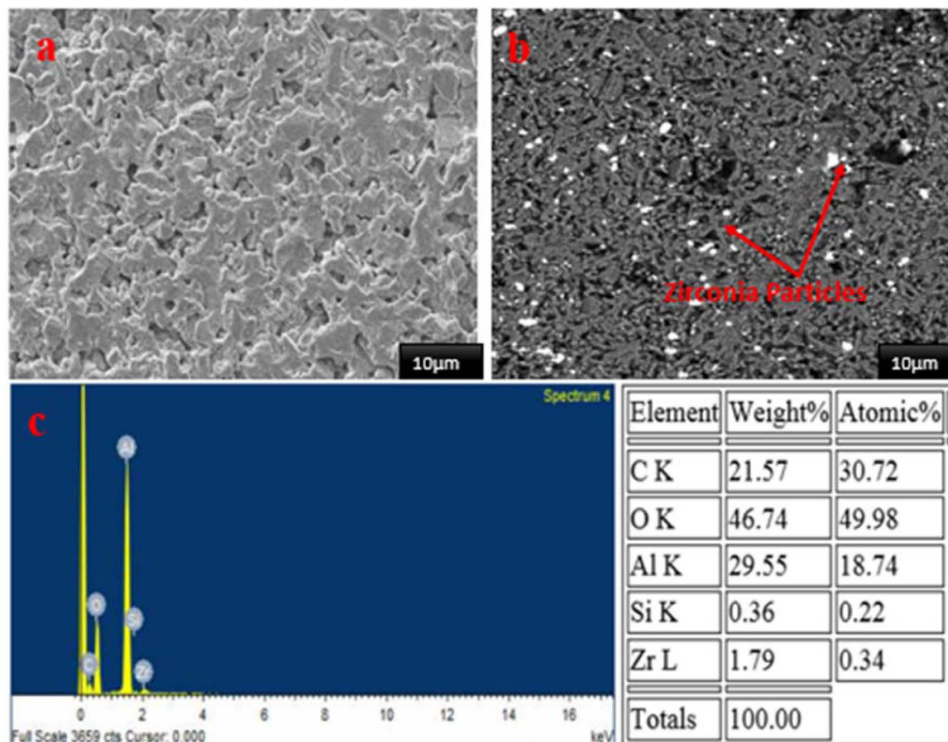


Fig. 4. SEM images and EDS Spectra shows the chemical composition of ZTA (a) SE (b) BSE (c) EDS analysis confirming composition.

sintering that reflects in high porosity value [33, 34]. Pores in SiC tend to be trapped in residues of sinter or inclusions. SiCA Pores have a much larger scale.

Fig. 3(a) shows that the grains of alumina appear to lose the distinctive feature of interconnected grain boundaries and sharp corners while Fig. 3(b) which is a BSE image shows very less porosity. Fig. 4 shows the development of sintered ZTA ceramics microstructure with increased zirconia material. The increasing content of zirconia is expected to increase the white component. With increasing concentration of zirconia, the degree of homogeneity in the microstructure of synthesized ZTA increases. The increasing proportions of alumina and zirconia in these composites are enriched. With the increase in zirconia material, the amount of open porosity appears to decrease [27, 28].

Fig. 4(a) shows the fine crystal structure and Fig. 4(b) clearly depicts that the ZrO_2 particles of different shape and size which are homogeneously dispersed in alumina matrix phase. Most of the particles are located at the grain boundaries [26]. The area of the surface formed a glassy phase between the ZTA matrixes (darker region). The SiC particles were uniformly distributed through the aluminium matrix in the alumina-SiC nanocomposite system as can be seen in Fig. 5. Largest proportions of SiC particles were identified in Al_2O_3 grains, while small numbers of big particles were observed at grain boundaries, resulting in the forming of fine alumina microstructures, and resulting in the pinning effects of SiC particles on Al_2O_3 grains. The

improvement in alumina mechanical performance is mainly due to the refining of their microstructural composition, while SiC inhibits alumina's grain limit mobility [35, 36].

Fig. 5(a) displays the glass penetrated samples surface area with the extra glass remaining on the surface. In Fig. 5(b) there is much porosity which confirms the porosity values measured. The blackish region clearly shows the porosity in SiCA samples.

Grain size distribution

The grain structure of matrix phase in simple alumina, ZTA, and SiCA was found with varying grain size, measured using SEM micrograph by ImageJ. The grain size for all the samples were found out in the range of 1-10 μm [7]. Micrographs of ZTA and SiCA shows elongated and eqiaxed grains respectively. ZTA showed mostly grains in the range of 1.5 μm with few larger particles while in case of SiCA the grain size measured is in the range of 2.5 to 6 μm . The small grains size of zirconia allows the retention of a larger amount of tetragonal phase in the alumina matrix which tends to inhibit the process of densification in the alumina matrix. Also, the grain size of simple alumina lies in the range of 5 to 8 μm .

It is clear that simple alumina has the variable grain size with mostly grains lying in the range of 5 to 8 μm with few larger grains also. The alumina grains are bimodal, and the use of zirconia as a second phase inhibits grain growth. The grain structure of alumina

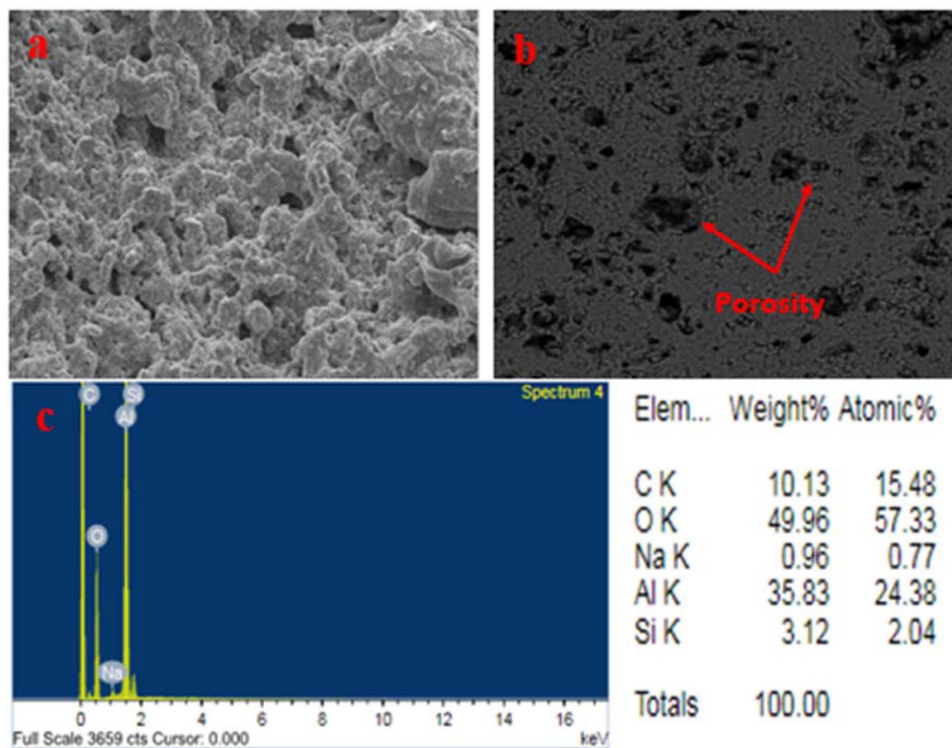


Fig. 5. SEM images and EDS Spectra shows the chemical composition of base alumina (a) SE (b) BSE (c) EDS analysis confirming composition.

matrix is larger, with elongated grains up to 10 μm grain size and a grain aspect ratio of around 2 μm [37]. ZTA showing mostly grains in the range of 1.5-2 μm with few larger particles. The small grains size of zirconia allows the retention of a larger amount of tetragonal phase in the alumina matrix which tends to inhibit the process of densification in the alumina matrix that results in high porosity value [33]. In case of SiCA the grain size measured is in the range of 2.5 to 6 μm. Most of the grains are found to be in this range. The large grain size resulted in decrease in hardness as a result of which toughness value will be increased.

SEM-EDX analysis of samples are investigated by using SEM for compositional Analysis. EDX analysis of the samples confirms the presence of ZrO₂ and SiC particles respectively as shown in Fig. 3(c)-5(c). The high percentage of carbon is due to the carbon tape and graphite electrode which was used for sputtering of samples so the electrons may pass through. The little percentage of oxygen is due to the no 100 percent inert atmosphere because nitrogen gas is used to create the inert atmosphere and that is not exactly to create inert atmosphere like noble gases. Fig. 3(c) showing the elemental composition of simple alumina samples. This analysis confirms the presence of alumina as the matrix phase as it has the second maximum percentage after oxygen. There is also the little amount of sodium (Na) which may be because of the deflocculating agent or from binder residue. The high percentage of carbon is mainly because of the sputtering media.

EDX analysis of ZTA (Fig. 4(c)) confirms the presence of zirconia as the second phase particle in alumina matrix. Again, the high percentage of carbon is because of sputtering and carbon tape. While the very little Si content is from Na₂SiO₃ which was used as doflocculant. Fig. 5(c) shows the EDX analysis of SiCA, Si content confirming its presence as the second phase particle in alumina while very little percentage of Na is because of sintering additives, i.e. Na₂CO₃ or Na₂CO₃.

Vickers hardness

Hardness was calculated at 980N. Five measurements were made at a distance of 3 mm using Eq. (6). Table 3 demonstrated the Vicker hardness value at given applied load. From the Table 3 it can be seen that SiCA shows the highest value of hardness at applied load

Table 3. Vickers hardness crack length and toughness measurements

Sample	Indentation diagonal a (um)	Crack length c (um)	Young Modulus GPa	Hardness GPa	Toughness MPa .m ^{0.5}
Alumina	417	541	270	18.53	3.5
ZTA	235	375	330	14.43	4.6
SiCA	344	440	410	22.89	2.7

because of coarser grain size. The main reason for this load is as we increase indentation load the hardness value decreases as evident by literature [5, 37]. Both ZTA and SiCA showed the same trend. This is due to indentation size effect (ISE) which results in incomplete and reversible deformation at low load. SiCA displayed the cracking which is due to the porosity value that made the indent too invisible at low loads.

Fig. 6 shows the Vickers hardness value of the samples. It can be seen that SiCA samples have the highest value of hardness because of the highest value of porosity while alumina sample has the lowest hardness value which is because of the densification as grain size in case of alumina is mostly in the range of 5-6 μm. ZTA samples have the intermediate values of hardness which is because of the very fine grain size and the grain size measured. The theoretic Vickers hardness value can be determined by the rule of mixture and hardness of fully dense Al₂O₃ and ZrO_{2.3} and it is estimated to be in the range between 16 and 17 GPa while the actually calculated hardness is 14.43 GPa. In short, the hardness value can be attributed to variation in grain size and porosity reported in literature [38-40].

Toughness test

Anstis method was used to calculate fracture toughness using Eq. (6) [37]. For fracture toughness evaluation indents with clear crack were measured as shown in Fig. 7. Crack size value will increase with load as suggested by researcher [18].

Fig. 7(a) shows the indentation in simple alumina while Fig. 7(b) showing the indentation in ZTA samples. The cracks on load of 1kgf in ZTA can clearly be seen. From the figure it can be seen that ZTA samples has shown resistance to indentation while the SiCA samples, Fig. 7(c) showed spalling and cracking. In addition, during indentation, residual stresses may also be produced that can accelerate crack growth and underestimate

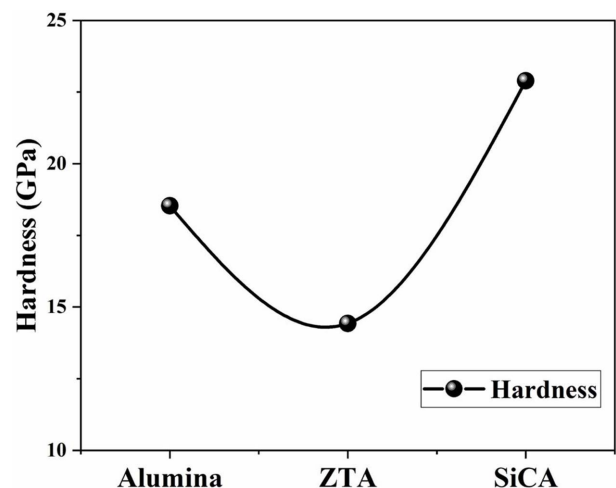


Fig. 6. Vickers hardness comparison plot.

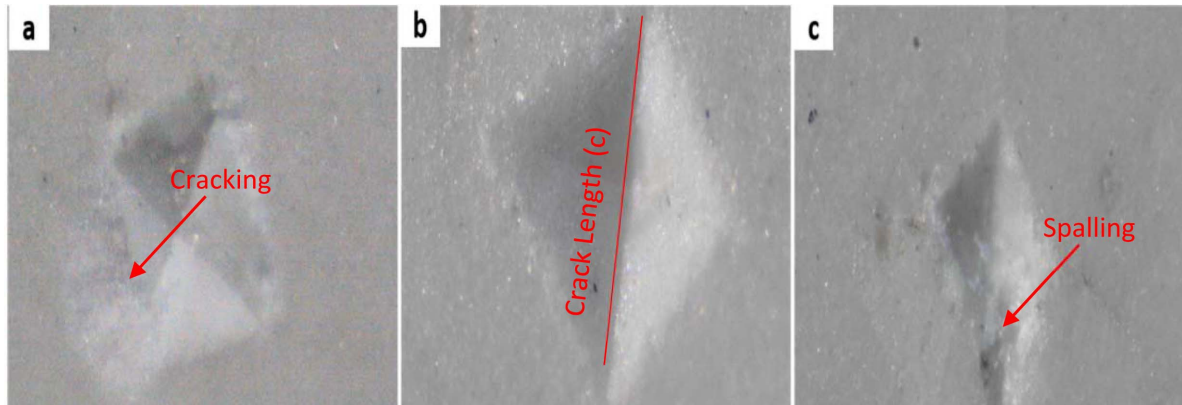


Fig. 7. Crack length of samples.

Table 4. Results comparison table

Reference	Compositions	Method	Tensile Strength	Hardness	Toughness MPa·m ^{0.5}
6	ZTA, CNTs	Injection molding	No Mechanical Characterization		
7	ZTA, SiC	Pressure less sintering	270-326 MPa	15.03	4.90
9	ZTA, Alumina	As received	274 MPa	16.9	–
10	Alumina, ZTA	Heat Treatment	–	12-13	4.5-4.9
13	Al ₂ O ₃ , SiC-Si ₃ N ₄ -Al ₂ O ₃	Hot Pressing, Pressure less sintering	–	12.3-15.6	For AZ 4.0
16	Alumina based	Pressing	195-221 MPa	13.314.8	–
21	Alumina, CNTs	Molecular level mixing	–	15-17	Alumina 2.90
29	95% alumina ceramic and 10% zirconia toughened alumina (ZTA)	Mixing, Sintering	0.667GPa	13.3-14.8	
This Work	Alumina, Reduced ZTA, Alumina/ SiC	Dry pressing	–	14.43	4.6

toughness of materials [41].

In case of SiCA it showed excessive cracking and spalling. The crack length *c* measured is the length from midpoint to tip of crack which was measured at average of 3mm. Crack size *c* and the relative toughness value for samples are given in Table 3. In table modulus

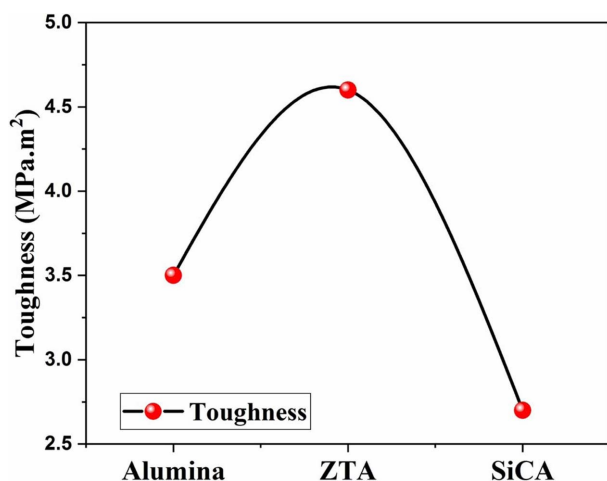


Fig. 8. Fracture toughness plot.

of elasticity for samples was taken from the literature which was 270 GPa for simple alumina 330 GPa for ZTA and 410 GPa for SiCA [42].

Fracture toughness values were measured using Eq. (7). Fig. 8 showing the toughness values of the samples. It is clear from the figure that ZTA samples showed maximum toughness value which is 4.6 MPa·m^{1/2} while simple alumina showed much lower value of fracture toughness. This toughness value is in agreement with previous study with zirconia content in the range of 0-20% [39]. The highest value of toughness of ZTA indicates that it has good resistance against projectile because of its lower density. ZTA also showed much better toughness than simple alumina which is because of the fine grain size and homogeneous dispersion of ZrO₂ in alumina matrix [43]. The calculated toughness is comparable table 4 with that of monolithic alumina, ZTA showed an increase of 82.6% [44].

Conclusion

Alumina reinforced with SiC and Zirconia ceramic matrix composite materials were successfully developed by using dry pressing method. Their microstructural

and mechanical properties were systematic studied, and a comparison was ZrO₂ made with other ceramic matrix composites. Improvement in densification was found by incorporation of SiC and Zirconia. It was observed that introduction of second phase particles like ZrO₂ and SiC not only downplaying of the grain size but also enhanced the fracture toughness value. The fracture toughness value of ZTA and SiCA was found higher than the simple alumina samples. On the other hand hardness value is decreased slightly but still comparable to other previously reported ceramic matrix composites.

Acknowledgment

This project was supported the Deanship of Scientific Research at Prince Sattam bin Abdul Aziz University, under the research project no. 2020/01/17063.

References

1. R.A. Malik, A. Hussain, T.K. Song, W.-J. Kim, R. Ahmed, Y.S. Sung, and M.-H. Kim, *Ceram. Int.* 43 (2017) S198-S203.
2. F. Akram, A. Hussain, R.A. Malik, T.K. Song, W.-J. Kim, and M.-H. Kim, *Ceram. Int.* 43 (2017) S209-S213.
3. A. Ullah, C.W. Ahn, R.A. Malik, and I.W. Kim, *Phys. B* 444 (2014) 27-33.
4. M. Raza, H. Alrobei, R.A. Malik, A. Hussain, M. Alzaid, M. Saleem, and M. Imran, *Metals*. 10[1] (2020) 1492.
5. O. Fakolujo, A. Merati, M. Bielawski, M. Bolduc, and M. Nganbe, *Ceram. Trans.* 249 (2014) 83-91.
6. R. Gadow, and F. Kern, *J. Ceram. Soc. Japan* 114[1335] (2006) 958-962.
7. O. Fakolujo, A. Merati, M. Bielawski, M. Bolduc, and M. Nganbe, *J. Mineral and Mater. Charact. Eng.* 4[1] (2016) 87-102.
8. W. Wang, J. Bi, K. Sun, M. Bu, N. Long, and Y. Bai, *J. Am. Ceram. Soc.* 94[11] (2011) 3636-3640.
9. S.G. Savio, V. Madhu, and A.K. Gogia, *Def. Sci.* 64[5] (2014) 477-483.
10. D. Casellas, M.M. Nagl, L. Llanes, and M. Anglada, *J. Mater. Process. Technol.* 143-144 (2003) 148-152.
11. T. Hotta, H. Abe, M. Naito, M. Takahashi, K. Uematsu, and Z. Kato, *Powder Technol.* 149[2-3] (2005) 106-111.
12. M.D. Barros, P.L. Rachadel, M.C. Fredel, R. Janssen, and D. Hotza, *J. Ceram. Sci. Technol.* 9[1] (2018) 69-78.
13. E. Medvedovski, *Ceram. Int.* 36[7] (2010) 2117-2127.
14. C. Kaufmann, D. Cronin, M. Worswick, G. Pageau, and A. Beth, *Shock Vib.* 10[1] (2003) 51-58.
15. E. Medvedovski, *Ceram. Int.* 36[7] (2010) 2103-2115.
16. M.V. Silva, D. Stainer, H.A. Al-Qureshi, O.R.K. Montedo, and D. Hotza, *J. Ceram.* 2014 (2014) 1-6.
17. I. Momohjimoh, M. A. Hussein, and N. Al-Aqeeli, *Nano-materials* 9[1] (2019) 86.
18. P.J. Hazell, C.J. Roberson, and M. Moutinho, *Mater. Des.* 29[8] (2008) 1497-1503.
19. F. Chen, S. Yang, J. Wu, J.-A. Galaviz-Perez, Q. Shen, J.M. Schoenung, E.J. Lavernia, and L. Zhang, *J. Am. Ceram. Soc.* 98[3] (2015) 732-740.
20. S.W. Kim, and K.A. Khalil, *J. Am. Ceram. Soc.* 89[4] (2006) 1280-1285.
21. S.I. Cha, K.T. Kim, K.H. Lee, C.B. Mo, and S.H. Hong, *Scr. Mater.* 53[7] (2005) 793-797.
22. G.-D. Zhan, J.D. Kuntz, J. Wan, and A.K. Mukherjee, *Nature Materials* 2[1] (2003) 38-42.
23. A.A. Mamedov, N.A. Kotov, M. Prato, D.M. Guldi, J.P. Wicksted, and A. Hirsch, *Nature Material* 1[3] (2002) 190-194.
24. R.H. Baughman, A.A. Zakhidov, and W.A. De-Heer, *Science* 297[5582] (2002) 787-792.
25. S.R. Bakshi, D. Lahiri, and A. Agarwal, *Int. Mater. Rev.* 55[1] (2010) 41-64.
26. M. Übeyli, R.O. Yildirim, and B. Ögel, *Mater. Des.* 28[4] (2007) 1257-1262.
27. X.F. Zhang, and Y.C. Li, *Mater. Des.* 31[4] (2010) 1945-1952.
28. X.F. Zhang, Y.C. Li, and S.J. Yu, *J. Exp. Mech.* 22 (2007) 631-6.
29. A. Harris, B. Vaughan, J. Yeomans, P. Smith, and S. Burnage, *Int. J. Appl. Ceram. Technol.* 14[3] (2017) 323-330.
30. J. Venkatesan, M.A. Iqbal, and V. Madhu, *Procedia Eng.* 173 (2017) 671-678.
31. C. Tallon, M. Limacher, and G.V. Franks, *J. Eur. Ceram. Soc.* 30[14] (2010) 2819-2826.
32. G.D. Quinn, *Ceram. Eng. Sci. Proc.* 27[3] (2008) 45-62.
33. T. Ostrowski, and J. Rodel, *J. Am. Ceram. Soc.* 82[11] (2004) 3080-3086.
34. B. Du, B. Zhao, and T. Duan, *Appl. Mech. Mater.* 143-144 (2012) 485-488.
35. J. Zhao, L.C. Stearns, M.P. Harmer, H.M. Chan, G.A. Miller, and R.E. Cook, *J. Am. Ceram. Soc.* 76[2] (1993) 503-510.
36. H.Z. Wang, L. Gao, and J.K. Guo, *Ceram. Int.* 26[4] (2000) 391-396.
37. O. Fakolujo, A. Merati, M. Bielawski, M. Bolduc, and M. Nganbe, *Ceram. Trans.* 249 (2014) 83-91.
38. I. Ganesh, G. Sundararajan, S.M. Olhero, and J.M. Ferreira, *Ceram. Int.* 37[3] (2011) 835-841.
39. J.J. Swab, *J. Appl. Ceram. Technol.* 1[3] (2004) 219-225.
40. D.R. Moore, *Int. J. Adhes. Adhes.* 28[4-5] (2008) 153-157.
41. A. Gubernat, L. Stobierski, and P. Labaj, *J. Eur. Ceram. Soc.* 27[2-3] (2007) 781-789.
42. M. Cegła, W. Habaj, and P. Podgórzak, *Probl. Mechatronics. Armament, Aviat. Saf. Eng.* 5[3] (2014) 23-34.
43. G.K. Bansal, W.H. Duckworth, and D.E. Niesz, *J. Am. Ceram. Soc.* 59[11-12] (1976) 472-478.
44. L. Curkovic, V. Rede, K.J. Grilec, and A. Mulabdic, in *Proceedings of the 12th Conference on Materials*, June 2007, p.40-45.